Table 5 Five Japanese institutions enrolled in this study

Institution	No. of enrolled patients ($N = 133$)	%
Aichi Cancer Center Hospital and Research Institute	29	21.8
Iwate Medical University Hospital	23	17.3
The Cancer Institute Hospital of Japanese Foundation for Cancer Research	20	15
National Cancer Center	26	19.5
Shizuoka Cancer Center	35	26.3

References

1. Becker G, Galandi D, Blum HE (2006) Malignant ascites: systematic review and guideline for treatment. Eur J Cancer 42:589–597
2. Smith EM, Jayson GC (2003) The current and future management of malignant ascites. Clin Oncol 15:59–72
3. Mamada Y, Yoshida H, Taniai N et al (2007) Peritoneovenous shunts for palliation of malignant ascites. J Nippon Med Sch 74(5):355–358
4. Zanon C, Grosso M, Aprà F et al (2002) Palliative treatment of malignant refractory ascites by positioning of Denver peritoneovenous shunt. Tumori 88:123–127
5. Tueche SG, Pector JC (2000) Peritoneovenous shunt in malignant ascites. The Bordet institute experience from 1975–1998. Hepatogastroenterology 47:1322–1324
6. Holm A, Halpern NB, Aldrete JS (1989) Peritoneovenous shunt for intractable ascites of hepatic, nephrogenic, and malignant ascites. Am J Surg 158:162–166
7. Qazi R, Savlov ED (1982) Peritoneovenous shunt for palliation of malignant ascites. Cancer 49:600–602
8. Adam RA, Adam YG (2004) Malignant ascites: past, present, and future. J Am Coll Surg 198(6):999–1011
9. Bieligk SC, Calvo BF, Coit DG (2001) Peritoneovenous shunting for gynecologic malignant ascites. Cancer 91(7):1247–1255
10. Edney JA, Hill A, Armstrong D (1989) Peritoneovenous shunts palliate malignant ascites. Am J Surg 158:598–601
11. Faught W, Kirkpatrick JR, Krepart GV et al (1995) Peritoneovenous shunt for palliation of gynecologic malignant ascites. J Am Coll Surg 180:472–474
12. Gough IR, Balderson GA (1993) Malignant ascites: a comparison of peritoneovenous shunting and nonoperative management. Cancer 71(7):2377–2382
13. Ginès P, Arroyo V, Vargas V et al (1991) Paracentesis with intravenous infusion of albumin as compared with peritoneovenous shunting in cirrhosis with refractory ascites. N Engl J Med 325(12):829–835
14. Seike M, Maetani I, Sakai Y (2007) Treatment of malignant ascites in patients with advanced cancer: peritoneovenous shunt versus paracentesis. J Gastroenterol Hepatol 22:2126–2166
15. Söderlund C (1986) Denver peritoneovenous shunting for malignant or cirrhotic ascites: a prospective consecutive series. Scand J Gastroenterol 21(10):1161–1172
16. Hyde GL, Eiseman B (1967) Peritoneal arterial shunt for intractable ascites. Arch Surg 95:369–373
17. Leveen HH, Christoudias G, Ip M et al (1974) Peritoneovenous shunting for ascites. Ann Surg 180:580–591
18. Lund RH, Newkirk JB (1979) Peritoneovenous shunting system for surgical management of ascites. Contemp Surg 14:31–45
19. Schumacher DL, Saclarides TJ, Staren ED (1994) Peritoneovenous shunts for palliation of the patient with malignant ascites. Ann Surg Oncol 1(5):378–381
20. Hussain FF, Meer ZF, Lopez AJ (2004) Peritoneovenous shunt insertion for intractable ascites: a district general hospital experience. Cardiovasc Intervent Radiol 27:325–328
21. Park JS, Won JY, Park SI et al (2001) Percutaneous peritoneovenous shunt creation for the treatment of benign and malignant refractory ascites. J Vasc Interv Radiol 12:1445–1448
22. Won JY, Choi SY, Ko H et al (2008) Percutaneous peritoneovenous shunt for treatment of refractory ascites. J Vasc Interv Radiol 19:1717–1722
23. Bratby MJ, Hussain FF, Lopez AJ (2007) Radiological insertion and management of peritoneovenous shunt. Cardiovasc Intervent Radiol 30:415–418
24. Cheung DK, Raaf JH (1982) Selection of patients with malignant ascites for a peritoneovenous shunt. Cancer 50:1204–1209
25. Moskovitz M (1990) The peritoneovenous shunt: expectations and reality. Am J Gastroenterol 82(8):917–929
26. Parsons SL, Watson SA, Steele RJ (1996) Malignant ascites. Br J Surg 83:6–14

International Journal of
Radiation Oncology
biology • physics

www.redjournal.org

Report

^{106}Ruthenium Plaque Therapy (RPT) for Retinoblastoma

Naoya Murakami, MD,* Shigenobu Suzuki, MD,† Yoshinori Ito, MD,* Ryoichi Yoshimura, MD, PhD,‡ Koji Inaba, MD,* Yuki Kuroda, MD,* Madoka Morota, MD, PhD,* Hiroshi Mayahara, MD, PhD,* Mototake Sakudo, MS,* Akihisa Wakita, MS,* Hiroyuki Okamoto, MS,* Minako Sumi, MD, PhD,* Yoshikazu Kagami, MD,* Keiichi Nakagawa, MD, PhD,§ Kuni Ohtomo, MD, PhD,§ and Jun Itami, MD, PhD*

*Departments of *Radiation Oncology and †Ophthalmic Oncology, National Cancer Center Hospital, Tokyo, Japan; ‡Department of Diagnostic Radiology and Oncology, Head and Neck Reconstruction Division, Graduate School, Tokyo Medical and Dental University, Tokyo, Japan; and §Department of Radiology, University of Tokyo Hospital, Tokyo, Japan*

Received Mar 13, 2011, and in revised form Oct 30, 2011. Accepted for publication Nov 1, 2011

Summary

One hundred one ^{106}ruthenium plaque therapies were retrospectively analyzed that were performed in 90 eyes of 85 patients with retinoblastoma between 1998 and 2008.

Purpose: To evaluate the effectiveness of episcleral ^{106}ruthenium plaque therapy (RPT) in the management of retinoblastoma.

Methods and Materials: One hundred one RPTs were retrospectively analyzed that were performed in 90 eyes of 85 patients with retinoblastoma at National Cancer Center Hospital between 1998 and 2008. Each RPT had a corresponding tumor and 101 tumors were considered in the analysis of local control. Median follow-up length was 72.8 months. Median patient age at the RPT was 28 months. Median prescribed doses at reference depth and outer surface of the sclera were 47.4 Gy and 162.3 Gy, respectively.

Results: Local control rate (LCR) and ocular retention rate (ORR) at 2 years were 33.7% and 58.7%, respectively. Unilateral disease, International Classification of Retinoblastoma group C or more advanced at the first presentation or at the time of RPT, vitreous and/or subretinal seeding, tumor size greater than 5 disc diameter (DD), reference depth greater than 5 mm, dose rate at reference depth lower than 0.7 Gy/hour, dose at the reference depth lower than 35 Gy, and (biologically effective dose with an α/β ratio of 10 Gy) at the reference depth lower than 40 Gy_{10} were associated with unfavorable LCR. Two patients died of metastatic disease. Radiation complications included retinal detachment in 12 eyes (13.3%), proliferative retinopathy in 6 (6.7%), rubeosis iris in 2 (2.2%), and posterior subcapsular cataract in 23 (25.6%).

Conclusion: RPT is an effective eye-preserving treatment for retinoblastoma.

Introduction

Retinoblastoma is the most common intraocular malignancy of childhood that arises from neuroepithelial cells of the retina. The reported incidence of retinoblastoma is 1 in 16,653-22,166 live births in Japan (1).

For the management of children with retinoblastoma, mutilating enucleation and external beam radiation therapy (EBRT) are

Reprint requests to: Naoya Murakami, MD, Department of Radiation Oncology, National Cancer Center Hospital, 5-1-1, Tsukiji Chuo-ku, Tokyo 104-0045, Japan. Tel: +[81]-3-3542-2511; Fax: +[81]-3-3545-3567; E-mail: namuraka@ncc.go.jp

Conflict of interest: none.

Int J Radiation Oncol Biol Phys, Vol. ■, No. ■, pp. 1–7, 2012
0360-3016/$ - see front matter
doi:10.1016/j.ijrobp.2011.11.002

employed with a decreasing frequency, because of the facial disfigurement and increased incidence of the secondary malignancies after EBRT (2). Chemotherapy has been replacing EBRT as the modality for organ preservation (3, 4). Although chemotherapy can shrink the retinoblastoma lesion, local therapy is indispensable to attain local control. Episcleral plaque brachytherapy has emerged as a treatment option as a focal therapy in the primary or secondary treatment of retinoblastoma (3-5). Low-energy gamma-ray emitting ^{125}I plaque is most used around the world, which is inexpensive and can be customized to fit each tumor shape by arranging seed locations in the episcleral applicator (5-7). In contrast, the pure beta ray-emitting ^{106}ruthenium (^{106}Ru) plaque is used mainly in Europe (8, 9). Although ^{106}Ru plaque is very expensive and cannot treat tumors with a height greater than 5-6 mm because it emits purely beta rays (energy 3.54 MeV) (8-11), the thickness of the applicators is only 1 mm in contrast to 3 mm thickness of the I-125 applicators, which is greatly advantageous when an infant's very small eyes are dealt with. In Japan, National Cancer Center Hospital is the only institution performing episcleral brachytherapy using ^{106}Ru plaque applicators. This retrospective study analyzes the results of ^{106}Ru plaque therapy (RPT) in the management of retinoblastoma.

Methods and Materials

We retrospectively reviewed the clinical records of all patients undergoing RPTs for retinoblastoma between December 1998 and November 2008 in the National Cancer Center Hospital, Japan. One hundred one tumors of 90 eyes in 85 patients were treated by RPT during this period. In 10 eyes, multiple tumors were treated by simultaneous application of the plaques. Local status of the 101 tumors could be evaluated. All tumors were followed at least for 1 year. Patient and tumor characteristics at the initial presentation are listed in Table 1. Tumor stage is based on International Classification of Retinoblastoma (ICRB) (4, 12, 13). Only 31 (30.7%) of the 101 tumors presented with confined diseases of group A or B. Vitreous and subretinal tumor seedings were seen in 41.6% and 35.6%, respectively.

When RPT was the initial treatment, it was considered as the first-line treatment. When RPT followed after local and/or systemic therapies that had successfully reduced the tumor, it was considered as the second-line treatment. RPT was considered as salvage therapy, provided that it was employed to treat a refractory or relapsed tumor after the preceding therapies. In the current series, RPT was employed in only 4 tumors as the first-line therapy. The other 62 tumors underwent RPT as the second-line therapy and 35 as salvage therapy (Table 2). Some too-large tumors, apparently not suitable to be treated by RPT, underwent RPTs, because there was a strong wish of the parents to conserve

Table 1 Characteristics of patients and 101 tumors at the initial presentation

Characteristics	Number
Patients	85
Gender	
Male	52
Female	33
Age at the first brachytherapy	28 mo (range 7-240)
Laterality	
Bilateral	60
Unilateral	25
Family history	
Positive	9
ICRB	
Group A	2 (2.0%)
Group B	29 (28.7%)
Group C	15 (14.9%)
Group D	43 (42.6%)
Group E	7 (6.9%)
Unknown	5 (5.0%)
Tumor with vitreous seeding	42 (41.6%)
Tumor with subretinal seeding	36 (35.6%)
Median tumor size	5 DD (range 0.8-20)

Abbreviations: DD = disc diameter; ICRB = International Classification of Retinoblastoma.

Table 2 Tumor and treatment characteristics at the 101 first RPTs

Tumor characteristics	Number (%)
First-line therapy	4 (4.0)
Second-line therapy	62 (61.4)
Salvage therapy	35 (34.6)
ICRB at brachytherapy	
Group A	9 (8.9)
Group B	29 (28.7)
Group C	20 (19.8)
Group D	37 (36.6)
Group E	6 (5.9)
Tumor with subretinal seeding	28 (27.7)
Tumor with vitreous seeding	42 (41.6)
Response to preceding therapy	
Good	34 (33.7)
Stable	41 (40.6)
Poor	17 (16.8)
Unknown	5 (5.0)
Tumor size (DD)	
Median	5 DD (range 0.5-22)
Brachytherapy dose at outer surface of sclera	
Median	162.3 Gy (range: 61.3-950.0)
Brachytherapy dose at outer surface of sclera (BED_3)	
Median	854.9 Gy_3 (range 101.2-4317.0)
Dose rate at outer surface of sclera	
Median	7.5 Gy/h (range 4.5-10.3)
Brachytherapy reference depth	
Median	5 mm (range 3-9)
Dose rate at reference depth	
Median	0.83 Gy/h (range 0.11-2.22)
Brachytherapy dose at reference depth	
Median	47.4 Gy (range 24.3-86.1)
Brachytherapy dose at reference depth (BED_{10})	
Median	65.6 Gy_{10} (range 27.0-131.3)
Brachytherapy treatment time	
Median	53.3 h (range: 20.5-332.3)

Abbreviations: BED = biological effective dose; DD = disc diameter; ICRB = the International Classification of Retinoblastoma; RPT = ruthenium plaque brachytherapy.

the eyes of their children. For far more advanced disease in which tumor spread toward anterior structures of the eye or infiltrates into the optic disc, and if a massive hemorrhage was developed in retina or vitreous space with a loss of vision, enucleation was employed with or without systemic chemotherapy according to the pathological risk features. Systemic chemotherapy regimen mostly used in this cohort was 3-drug chemotherapy with carboplatin, etoposide, and vincristine.

Tumor response to the preceding therapies was defined as follows. The tumor whose stage attained down-grouping was classified as a good response, up-grouping as a poor response, and no group change as stable.

All episcleral ^{106}Ru plaque applicators (BEBIG Isotopen und Medizintechnik GmbH, Berlin, Germany) were inserted under general anesthesia. Before the operation, tumor location and height were assessed by slit lamp examinations with or without ultrasound and an appropriate plaque was selected. The plaques are hemispherically shaped with radii of 12 and 14 mm. CIA and CIB are used to treat anteriorly located tumor because they are semicircularly shaped concave in order to avoid cornea. COC are used to treat the tumor located in the posterior pole with a notch to avoid optic disc. CCA and CCB are round shaped and used to treat tumors which are away from cornea or optic disc. The diameters of A and B are 15.5 mm and 20 mm, respectively. To insert the plaques, extraocular muscles were separated temporarily. The selected plaques were sutured through the plaque eyelets to the sclera surface. The plaques were removed also under general anesthesia after the planned duration of radiation. The duration of radiation was calculated to administer prescription dose of 40 Gy to the reference depth. The reference depth was the height of tumor plus sclera thickness (1 mm) with a safety margin of 1 mm. Lateral tumor margin was set to 2-3 mm (10). Before July 2005, reliable ultrasound was not available to determine tumor height; therefore, the slit lamp was used to estimate it using its focus. Therefore before July 2005, only tumor width expressed by disc diameter (DD) and reference depths diagnosed approximately by slit lamp were available in the medical records. And for tumors with vitreous seeding, reference depth was set to 5-6 mm, which was regarded as the limit of the range of RPT. Hence, tumors with vitreous seeding without description of reference depth in medical record could be recalculated as having a reference depth of 5-6 mm. Before September 2006, the reference depth was 5 mm and thereafter it was set to 6 mm because of the dose tables provided by the manufacturer. Since May 2002, BEBIG has delivered its ^{106}Ru eye plaques with new protocols of radioactivity measurements in accordance with the National Institute of Standards and Technology calibration system. Therefore recalculations were performed for this study to correct the prescribed dose before the introduction of the new calibration system by using the conversion factor table provided by BEBIG (14). Because most of the conversion factors, which differ by applicator type and reference depth, were greater than 1.0, median dose at the reference depth became greater than 40 Gy after the recalculation (Table 2).

Because the biological effect of RPT could differ by dose rate and combined effect with EBRT must be considered, biologically effective dose (BED) was calculated according to the method of Dale (15) and is given by

$$\mathrm{BED} = \text{Total dose} \times 1 + \frac{2\mathrm{R}}{\mu}\left(\frac{\beta}{\alpha}\right)\{1 - 1/\mu\mathrm{T}[1 - \exp(-\mu T)]\}$$

where R indicates dose rate, T the treatment time, and μ the repair rate constant of sublethal damage. The value of μ was assumed as 0.46 hour^{-1} (corresponding to repair half time of 1.5 hours) (15). The α/β values used in this analysis were α/β = 10 Gy for tumor control and α/β = 3 Gy for late normal tissue morbidities. In 85 of 101 RPTs, the reference depth and prescribed dose could be obtained and BED_{10} (BED with an α/β ratio of 10 Gy) could be calculated. Because the outer surface of the sclera directly touches the plaque applicator (depth 0 mm), dose and BED_3 (BED with an α/β ratio of 3 Gy) of the outer surface of sclera could be calculated for 97 procedures whose applicator type and treatment time were known. For deriving total BED_3 of outer surface of sclera, BED_3 of EBRT, if any, before and after the RPT was added. In 16 eyes in which part of retina had overlapping multiple RPTs, BED_3 of outer surface of sclera of each RPT was added.

Ophthalmologic follow-up was performed with examinations under anesthesia every 1-2 months after the therapy until tumor control was achieved. Thereafter, examinations were performed every 2-6 months as needed.

The probabilities of local control rate (LCR), ocular retention rate (ORR), and overall survival (OS) were calculated using the Kaplan-Meyer method (16). For LCR, 101 tumors treated by 101 RPTs were taken into account. Local control was assessed by retinal diagram before and after the RPTs. Tumor persistent or regrowing within margins of the retina covered by the plaque applicator was considered as local failure. For the estimate of ORR, enucleation from disease progression or treatment-related complications and death from any causes were scored as an event and 90 eyes were subjects of the analysis. ORR was calculated from date of the last RPT to date of the events or to the last follow-up. The relationships between clinical and treatment variables and LCR were analyzed by the univariate and multivariate analyses. A P value of $<.05$ was considered statistically significant. The continuous variables were dichotomized to give the lowest P values in the log-rank test. The variables with P values $<.05$ were further analyzed in multivariate analysis by Cox proportional hazards test.

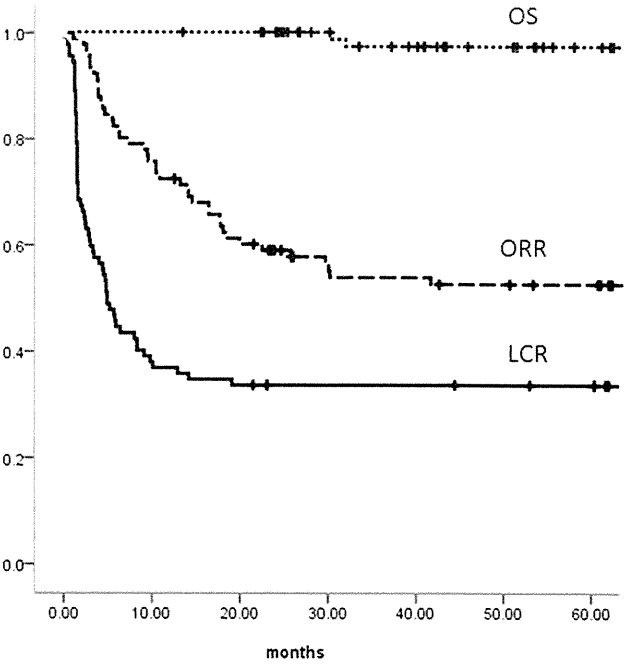

Fig. 1. Kaplan-Meyer curves of local control rate (LCR), ocular retention rate (ORR), and overall survival (OS).

Results

Tumor and treatment characteristics at the 101 RPTs were summarized in Table 2. Median patient follow-up length was 72.8 months (range 12.2-130). LCR of the 101 tumors treated by the 101 RPTs was 33.7% in 2 years with 31 tumors controlled (Fig. 1). All local failures were seen within 24 months after RPTs. The locally failed tumors were managed by various modalities including repeated RPT. Forty-two eyes (46.7%) were enucleated during the follow-up period and estimated 2 and 4 years ORR rates are 58.7% and 52.2%, respectively (Fig. 1).

Univariate analysis revealed clinical and treatment factors related with LCR (Table 3). Unilateral disease, ICRB group C or more at the presentation or at the time of RPT and vitreous seeding/subretinal seedings at the time of RPT, tumor size greater than 5 DD, dose at the reference depth lower than 35 Gy, BED_{10} for the reference depth lower than 40 Gy_{10}, reference depth greater than 5 mm, and dose rate at reference depth lower than 0.7 Gy/hour were associated with unfavorable LCR. Multivariate analysis revealed that ICRB group C or more at the initial presentation or at the time of RPT, and BED_{10} for the reference depth tumor lower than 40 Gy_{10} were statistically significant predictive factors for unfavorable LCR (Table 3). The tumors were classified into 2 groups according to the ICRB and BED_{10} for reference depth (BED_{10}). Group 1 was defined as ICRB A/B both at initial presentation and at RPT and BED_{10} for the reference depth $\geqq 40$ Gy_{10}. All other tumors were classified into group 2. There were 17 tumors in group 1 and 71 in group 2. Sixteen RPTs and 5 tumors lack the information of reference depth and initial ICRB, respectively. But if the tumor ICRB was not A/B at the time of RPT, it could be classified as group 2 even if neither reference depth nor initial ICRB were unknown. Therefore total number included in this grouping was above 85 but below 101. Two-year LCR were 64.7% and 25.4% in group 1 and group 2, respectively, with a statistical significant difference (Fig. 2). During the follow-up period, 2 patients died of brain metastasis with 3-year OS rate of 97.3% (Fig. 1).

As for morbidities, in 1 case, sclera ruptured during the operation, which required systemic chemotherapy but resulted in chemotherapy-refractory relapse and eventual enucleation. Twelve eyes (13.3%) developed retinal detachment, 6 eyes (6.7%) proliferative retinopathy, and 2 eyes (2.2%) rubeosis with abnormal neovascularization of iris. Both eyes with rubeosis eventually were enucleated because of glaucoma or disease progression. Twenty-three (25.6%) of 90 eyes developed posterior subcapsular cataract and 6 eyes required surgery for cataract. Median interval to cataract development after RPT was 35.0 months (range 0-87.33). Posterior subcapsular cataract development related only with whether or not EBRT was performed during the entire clinical course with cataract occurring in 28.1% of the patients undergoing EBRT at 3 years and 2.9% of those without EBRT ($P=.033$) (Fig. 3a). Thirty-four eyes (37.8%) had a retinal and vitreous hemorrhage after RPT. The incidence of retinal detachment, proliferative retinopathy, and rubeosis showed a correlation with radiation dose of the outer surface of sclera. $BED_3 \geqq 1200$ Gy_3 of the outer surface of sclera was significantly associated with a higher incidence either of retinal detachment, proliferative retinopathy or rubeosis ($P=.017$) (Fig. 3b).

There were 2 enucleations without tumor progression—1 of which developed after circulatory collapse of the retina after repeated selective ophthalmic arterial infusions (17) and transpupillary thermotherapy (18) for posterior pole of the retina. The other developed rubeosis iris caused by RPT as mentioned previously.

Two patients had a second malignancy after RPT. Both patients had hereditary retinoblastoma and 1 had family history of retinoblastoma. Both patients received EBRT and 1 had also received chemotherapy. One patient developed rhabdomyosarcoma in the nasal cavity within EBRT radiation field 27 months after the EBRT and 6 months after the RPT. The other had Ewing sarcoma in right mandible outside of EBRT fields 89 months after the EBRT and 76 months after RPT.

Discussion

In this study, we reported treatment results for RPTs for 101 retinoblastomas in 90 eyes of 85 patients in 10 years.

LCR of EBRT was reported to be 31%-64% (19, 20). Although small tumors could be controlled by 40-46 Gy of conventional fractionated EBRT, the control rate of greater tumors was unsatisfactory. Recently, 2 retrospective studies of RPT for retinoblastoma have been published (8, 9). Schueler et al (8) achieved excellent results of 92.9% LCR and eyes could be preserved in 88.6%. Abouzeid et al (9) also showed good results of 59%-73% eye preservation rate. Another radionuclide of ^{125}I also attained an excellent LCR ranging between 83% and 95% (6, 7). The prescribed dose of ^{125}I plaque brachytherapy was 40 Gy (6, 7) but those of RPT has not yet been standardized. In the study of Schueler et al (8) using the National Institute of Standards and Technology dosimetry standard, the dose at the apex ranged from 53-233 Gy and a mean dose extended up to 138 Gy with an estimated accuracy of no better than $\pm 35\%$. They concluded that the recommended dose should be 88 Gy at the tumor apex, although they mentioned the possibility of dose de-escalation (8). On the other hand, Abouzeid et al (9) prescribed 50 Gy at the tumor apex and found that the apical dose was not a predictive factor of local failure. They concluded that favorable tumor control could be achieved with a median dose at the tumor apex of 51.7 Gy. In this study, recalculated median dose at the tumor apex was 47.4 Gy (range 24.3-86.1 Gy) and comparable to that of Abouzeid et al (9). However, 2-year LCR of the current study was 33.7% and inferior to the other studies of RPT. The unfavorable LCR can be explained by the facts that 62.3% of the patients belonged to ICRB group C or more with unfavorable factors of vitreous seeding or subretinal seedings in the current study. In contrast, other studies included only the patients with tumors up to ICRB group C with a limited vitreous seedings. However, it has to be emphasized that as shown in Table 3, even with the presence of vitreous seedings about 20% of tumors could be controlled by RPT. Although tumor control rate of RPT with unfavorable factors were dismal, progressed tumors could be ultimately salvaged by enucleation without risking survival; therefore, it is meaningful to try to treat advanced tumors with a conservative approach including RPT especially for the patients whose contralateral eye had already been enucleated. As shown in Fig. 2, LCR for tumors without unfavorable factors were comparable to the other series (8, 9).

Factors that influenced LCR were disease laterality, ICRB, vitreous/subretinal seeding, tumor size, reference depth, dose, and dose rate at reference depth. It was in accordance with other reports that pointed out that vitreous seeding, subretinal seeding, and dose at the tumor apex were prognostic factors of local

Table 3 Univariate and multivariate analysis of potential predictive factors influencing LCR*

	LCR					
Factors	2-y	*P* value in uni	*P* value in multi	Hazard ratio	95% CI	
Gender						
Male	36.2	.462				
Female	29.4					
Laterality						
Bilateral	38.9	.017*	.133			
Unilateral	15.0					
ICRB at initial presentation						
Group A/B	53.3	.022*	.001*	10.323	2.737	38.932
Group C/D/E	24.1					
ICRB at brachytherapy						
Group A/B	55.9	<.001*	.027*	0.441	0.213	0.911
Group C/D/E	20.7					
Applicator type						
CIA/CCA	42.1	.141				
CIB/CCB	26.0					
Prior EBRT						
Yes	32.0	.707				
No	35.7					
Treatment type						
First-line/second-line	27.1	.152				
Salvage	45.5					
Vitreous seeding at brachytherapy						
Yes	18.9	.016*	.892			
No	43.6					
Subretinal seeding at brachytherapy						
Yes	19.2	.04*	.785			
No	39.4					
Response to preceding therapy						
Good	43.8	.116				
Stable/poor	28.6					
Tumor size at brachytherapy (DD)						
<5 DD	52.5	.001*	.252			
≧5 DD	19.6					
Dose rate at outer surface of sclera						
<3 Gy/h	29.5	.271				
≧3 Gy/h	36.4					
Reference depth						
<5 mm	47.1	.01*	.295			
≧5 mm	21.4					
Dose rate at reference depth						
<0.7 Gy/h	17.9	.011*	.105			
≧0.7 Gy/h	40.4					
Dose at reference depth (Gy)						
<35 Gy	11.8	.008*	.448			
≧35 Gy	37.9					
Dose at reference depth (BED_{10})						
<40 Gy_{10}	0.0	.001*	.034*	2.237	1.063	4.710
≧40 Gy_{10}	36.9					
Treatment time						
<53 h	37.8	.195				
≧53 h	29.8					

Abbreviations: BED = biological effective dose; CCA = ■; CI = confidence interval; CIA = ■; CIB = ■; CBB = ■; DD = disc diameter; EBRT = external beam radiation therapy; ICRB = the International Classification of Retinoblastoma; LCR = local control rate; multi = multivariate analysis; uni = univariate analysis.

* $P<.05$.

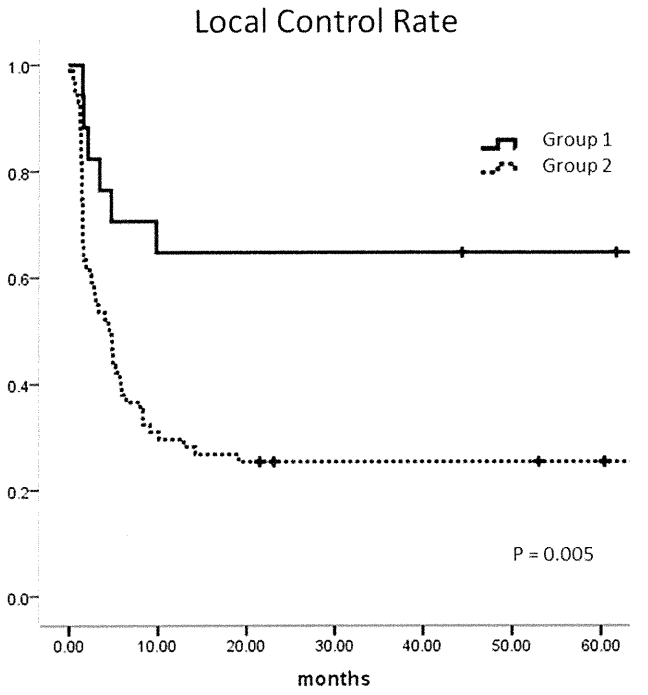

Fig. 2. Local control rate (LCR) according to the group classification by the International Classification of Retinoblastoma and biological effective dose (BED) with $\alpha/\beta = 10$ Gy of the reference depth (for details refer to the text).

control. Both reference depth and dose rate at reference depth were prognostic factors of local control suggesting that physical limitation of RPT, which is not suitable for treating tall tumors as previously reported (8-11).

The administration of previous EBRT did not influence LCR (Table 3), suggesting that response to RPT did not differ between relapsed or refractory tumors after EBRT and radiation-naive tumors as previously reported (9).

Concerning the morbidities, the incidence of posterior subcapsular cataract was influenced by EBRT but not by RPT whose dose to the lens is negligible. In the current study, the incidence of proliferative retinopathy was as low as 6.7%, which is similar to the low reported incidence of 2.4% in Abouzeid's study. In contrast, the incidence was reported to be as high as 17.1% in the series by Schueler et al in which a higher dose was employed. Proliferative retinopathy has been reported to occur in 13%-19% after ^{125}I plaque brachytherapy in which dose reached further than ^{106}Ru.

$BED_3 \geqq 1200$ Gy_3 of the outer surface of sclera was significantly correlated with the incidence of either retinal detachment or proliferative retinopathy or rubeosis (Fig. 3b). A higher dose for sclera was demonstrated to cause late complications associated with RPT; therefore, it is important to exclude tall tumors whose dose of the outer surface of sclera will be high in order to avoid complications. However, there were only 2 enucleations caused by the late complications of RPT, and RPTs were generally well tolerated.

There were 2 secondary malignancies in the current series. Both of them occurred in the patients with a hereditary retinoblastoma, 1 of them developed within the EBRT fields. In accordance with the literature (6, 7), plaque brachytherapy itself did not seem to increase the incidence of secondary malignancy.

Conclusion

RPT is an effective and safe focal therapy for retinoblastoma. However, optimal dose of RPT remains to be studied further.

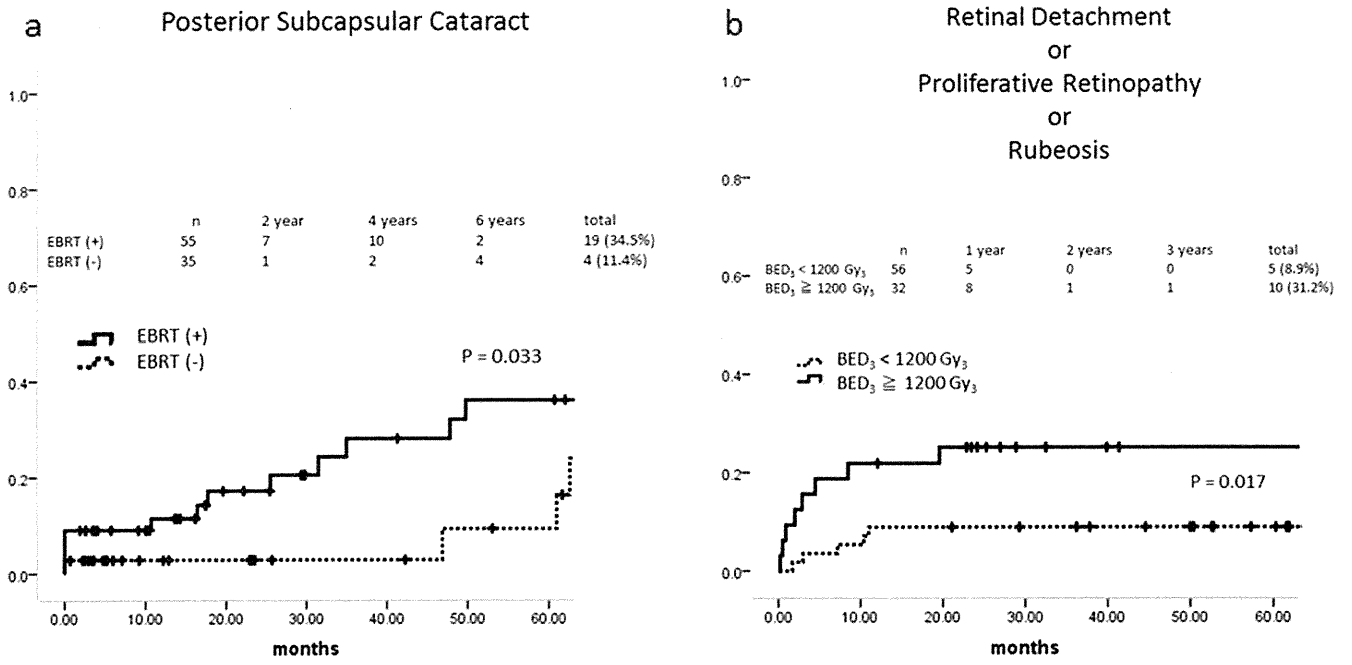

Fig. 3. (a) Cumulative incidence of posterior subcapsular cataract according to whether external beam radiation therapy (EBRT) was administered. (b) Cumulative incidence of retinal detachment, proliferative retinopathy and rubeosis stratified by biological effective dose (BED) with $\alpha/\beta = 3$ Gy at the outer surface of sclera.

References

1. National registry of retinoblastoma in Japan (1975–1982). The Committee for the National Registry of Retinoblastoma. *Nippon Ganka Gakkai Zasshi* 1992;96:1433-1442.
2. Kleinerman RA, Tucker MA, Tarone RE, et al. Risk of new cancers after radiotherapy in long-term survivors of retinoblastoma: an extended follow-up. *J Clin Oncol* 2005;23:2272-2279.
3. Abramson DH, Schefler AC. Update on retinoblastoma. *Retina* 2004; 24:828-848.
4. Lin P, O'Brien JM. Frontiers in the management of retinoblastoma. *Am J Ophthalmol* 2009;148:192-198.
5. Freire JE, De Potter P, Brady LW, et al. Brachytherapy in primary ocular tumors. *Semin Surg Oncol* 1997;13:167-176.
6. Shields CL, Shields JA, Cater J, et al. Plaque radiotherapy for retinoblastoma: long-term tumor control and treatment complications in 208 tumors. *Ophthalmology* 2001;108:2116-2121.
7. Shields CL, Mashayekhi A, Sun H, et al. Iodine 125 plaque radiotherapy as salvage treatment for retinoblastoma recurrence after chemoreduction in 84 tumors. *Ophthalmology* 2006;113:2087-2092.
8. Schueler AO, Fluhs D, Anastassiou G, et al. Beta-ray brachytherapy with 106Ru plaques for retinoblastoma. *Int J Radiat Oncol Biol Phys* 2006;65:1212-1221.
9. Abouzeid H, Moeckli R, Gaillard MC, et al. (106)Ruthenium brachytherapy for retinoblastoma. *Int J Radiat Oncol Biol Phys* 2008;71: 821-828.
10. Nag S, Quivey JM, Earle JD, et al. The American Brachytherapy Society recommendations for brachytherapy of uveal melanomas. *Int J Radiat Oncol Biol Phys* 2003;56:544-555.
11. Jarvien H, Cross WG, Soares C, et al. Dosimetry of beta rays and low-energy photons for brachytherapy with sealed sources. *J ICRU* 2004;4: 2-175.
12. Linn Murphree A. Intraocular retinoblastoma: the case for a new group classification. *Ophthalmol Clin North Am* 2005;18:41-53. viii.
13. Shields CL, Mashayekhi A, Au AK, et al. The International Classification of Retinoblastoma predicts chemoreduction success. *Ophthalmology* 2006;113:2276-2280.
14. BEBIG. BEBIG Ruthenium Augenapplikatoren Kundeninformation: Einführung der neuen NIST-kalibrierten Dosimetrie Einführung der neuen PTB-kalibrierten Aktivitätsmessungen. 2002:version 1.03 v. 12.11.02.
15. Dale RG. The application of the linear-quadratic dose-effect equation to fractionated and protracted radiotherapy. *Br J Radiol* 1985;58:515-528.
16. Kaplan EL, Meier P. Nonparametric estimation from incomplete observations. *J Am Stat Assoc* 1958;53:457-481.
17. Yamane T, Kaneko A, Mohri M. The technique of ophthalmic arterial infusion therapy for patients with intraocular retinoblastoma. *Int J Clin Oncol* 2004;9:69-73.
18. Oosterhuis JA, Journee-de Korver HG, Kakebeeke-Kemme HM, et al. Transpupillary thermotherapy in choroidal melanomas. *Arch Ophthalmol* 1995;113:315-321.
19. Foote RL, Garretson BR, Schomberg PJ, et al. External beam irradiation for retinoblastoma: patterns of failure and dose-response analysis. *Int J Radiat Oncol Biol Phys* 1989;16:823-830.
20. Hernandez JC, Brady LW, Shields JA, et al. External beam radiation for retinoblastoma: results, patterns of failure, and a proposal for treatment guidelines. *Int J Radiat Oncol Biol Phys* 1996;35: 125-132.

Japanese Journal of Clinical Oncology Advance Access published April 23, 2012

JJCO Japanese Journal of Clinical Oncology

Jpn J Clin Oncol 2012
doi:10.1093/jjco/hys055

Case Report

Successful Control of Intractable Hypoglycemia Using Radiopharmaceutical Therapy with Strontium-89 in a Case with Malignant Insulinoma and Bone Metastases

Atsushi Naganuma[1,2], Hiroshi Mayahara[3], Chigusa Morizane[1,*], Yuriko Ito[1,4], Atsushi Hagihara[1,5], Shunsuke Kondo[1], Hideki Ueno[1], Jun Itami[3] and Takuji Okusaka[1]

[1]Hepatobiliary and Pancreatic Oncology Division, National Cancer Center Hospital, Tokyo, [2]Department of Gastroenterology, Takasaki General Medical Center, National Hospital Organization, Gunma, [3]Radiation Oncology Division, National Cancer Center Hospital, Tokyo, [4]Department of Clinical Oncology, Yamagata University School of Medicine, Yamagata and [5]Department of Hepatology, Osaka City University Graduate School of Medicine, Osaka, Japan

*For reprints and all correspondence: Chigusa Morizane, Hepatobiliary and Pancreatic Oncology Division, National Cancer Center Hospital, 5-1-1 Tsukiji, Chuo-ku, Tokyo 104-0045, Japan. E-mail: cmorizan@ncc.go.jp

Received December 21, 2011; accepted March 22, 2012

This report describes the case of a 57-year-old woman with liver and bone metastases from malignant insulinoma, who was afflicted with severe hypoglycemia. Treatment of the liver metastases using octreotide, diazoxide and transarterial embolization failed to raise her blood glucose level and she required constant glucose infusion (about 1000 kcal/day) and oral feeding (about 2200 kcal/day) to avoid a hypoglycemic attack. Subsequently, 110 MBq (2.0 MBq/kg) of strontium-89 were administered by intravenous injection. Three weeks after the strontium-89 injection, we could reduce the dose of constant glucose infusion while maintaining a euglycemic status. Six weeks after the injection, the constant glucose infusion was discontinued. Although strontium-89 therapy is indicated for patients with multiple painful bone metastases, it was also useful as a means of inhibiting tumor activity and controlling hypoglycemia in this case. To our knowledge, this is the first report to provide evidence that strontium-89 can be useful in controlling intractable hypoglycemia in patients with malignant insulinoma with bone metastases.

Key words: strontium-89 – malignant insulinoma – bone metastases

INTRODUCTION

Insulinomas are rare tumors that arise from the pancreatic islet cells that produce insulin. Approximately 5–10% of the insulinomas are cancerous (1). It is often difficult to control inappropriate insulin secretion and hypoglycemia in patients with a malignant insulinoma. Although surgery is indicated for symptomatic or malignant insulinoma, only medical therapy is suggested for unresectable patients (2). Some cases suffer from intractable hypoglycemia as a result of the limited efficacy of medical therapy. We report here on the case of a 57-year-old woman with a malignant insulinoma and bone metastases in whom intractable hypoglycemia was successfully controlled by using radiopharmaceutical therapy with strontium (Sr)-89.

CASE REPORT

In March 2002, a 57-year-old woman experienced frequent hypoglycemic attacks and was diagnosed as having an insulinoma of the pancreas tail at a previous hospital. She

underwent surgery including a distal pancreatectomy and splenectomy at the previous hospital. The maximum diameter of the surgically removed tumor was 10 cm. The histopathological findings revealed a pancreas islet cell carcinoma. The tumor had directly invaded the spleen and protruded into the splenic vein and pancreatic duct. The surgical resection stump was negative.

In February 2005, multiple liver metastases were detected and the patient was referred to our hospital. Then, she received a partial hepatectomy for multiple liver metastases in our hospital. The histopathological findings of resected specimen showed a low-grade endocrine cell carcinoma. The immunohistochemical staining showed positive for chromogranin A and synaptophysin, but it showed negative for insulin. In July 2006, she underwent a second partial hepatectomy for recurrent multiple liver metastases. Histopathological examination of the liver metastases showed similar findings to the first liver segmental resection.

In December 2008, multiple liver metastases and multiple bone metastases including lumbar vertebrae and iliac bone were detected. In March 2009, she started zoledronic acid hydrate treatment for the bone metastases, but it was discontinued because of severe jaw pain suggesting the possibility of mandibular osteonecrosis. In November 2009, the patient experienced a hypoglycemic attack again. The patient was hospitalized to control her serum glucose level. The laboratory data obtained at admission are shown in Table 1. Regarding the serum hormonal level, the insulin level was slightly elevated but the glucagon level was not elevated. The level of neuron-specific enolase was slightly elevated. The patient underwent short-acting somatostatin analogs for 14 days to control the serum glucose level due to their antiproliferation effect. After having confirmed that there was no worsening of the hypoglycemia symptoms, we changed her treatment to a long-acting somatostatin analog (Sandostatin-LAR; Novartis Pharmaceuticals). However, hypoglycemia occurred frequently (Fig. 1) even after the initiation of octreotide therapy. The patient refused to continue the octreotide therapy because her hypoglycemic attacks had not improved. The hypoglycemia persisted after the discontinuation of octreotide. Next, diazoxide was administered with no effect but with the side effects of significant edema and weight gain. We decided to undertake transarterial embolization (TAE) to necrotize the liver metastases and

Table 1. Laboratory data upon the first admission after the experience of a hypoglycemic attack

	Actual level	Normal level		Actual level	Normal level
Hematology			Tumor markers		
Leukocyte (per mm^3)	10 200	(3900–6300)	CEA (ng/ml)	2.5	(<5)
Hemoglobin (g/dl)	11.9	(11.3–14.9)	CA19–9 (U/ml)	12	(<37)
Platelet (per mm^3)	39×10^4	($12.5–37.5 \times 10^4$)	NSE (ng/ml)	18.5 (H)	(<15)
Biochemistry			ProGRP (pg/ml)	37.7	(<46)
Total protein (g/dl)	8.0	(6.3–8.3)	Hormones		
Albumin (g/dl)	3.6(L)	(3.7–5.2)	Insulin (mIU/ml)	12.9 (H)	(1.84–12.2)
Total bilirubin (mg/dl)	0.6	(0.3–1.2)	Gastrin (pg/ml)	82	(<200)
Fasting glucose (mg/dl)	70	(69–104)	Glucagon (pg/ml)	120	(50–150)
BUN (mg/dl)	14	(8–22)	Urine		
Creatine (mg/dl)	0.6	(0.4–0.7)	pH	6.0	(4.6–7.5)
Sodium (mEq/l)	138	(138–146)	Protein	(—)	
Potassium (mEq/l)	4.2	(3.6–4.9)	Sugar	(—)	
Chloride (mEq/l)	104	(99–109)	Blood	(—)	
Calcium (mg/dl)	9.0	(8.7–10.3)			
Amylase (IU/l)	64	(42–132)			
ALP (IU/l)	440 (H)	(115–359)			
AST (IU/l)	16	(13–33)			
ALT (IU/l)	9	(6–27)			
LDH (IU/l)	174	(119–229)			
γ-GTP (IU/l)	25	(10–47)			

BUN, blood urea nitrogen; ALP, alkaline phosphatase; AST, aspartate aminotransferase; ALT, alanine aminotransferase; LDH, lactate dehydrogenase; γ-GTP, γ-glutamyltransferase; APTT, activated partial thromboplastin time; CEA, carcinoembryonic antigen; CA19-9, carbohydrate antigen 19-9; NSE, neuron-specific enolase; Pro-GRP, pro-gastrin-releasing peptide; (H), high; (L), low.

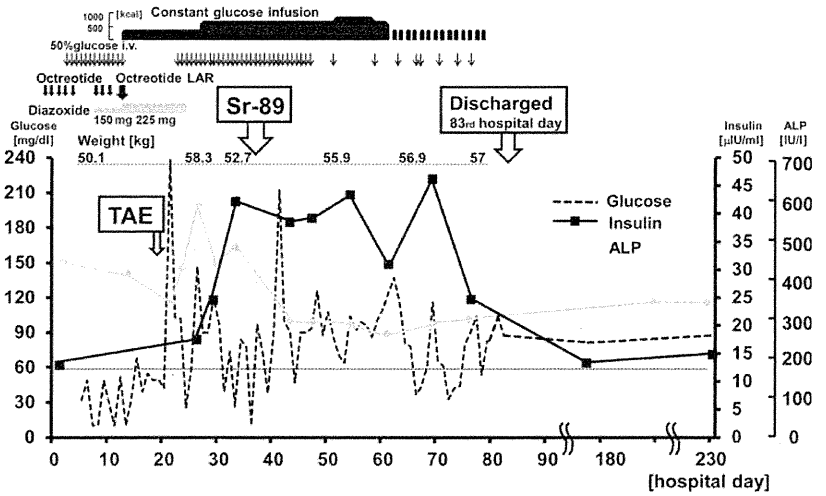

Figure 1. Clinical course. Three weeks after the strontium-89 injection, the patient was weaned from the constant glucose infusion while successfully maintaining euglycemia and lower circulating insulin levels. About 6 weeks after the injection, the constant glucose infusion was completely stopped, even though the previous treatment had failed.

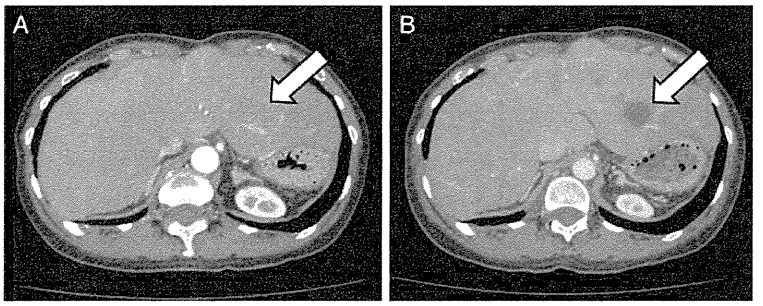

Figure 2. Liver metastases were observed using enhanced computed tomography (A and B, arrow). The liver metastases did not exhibit remarkable hypervascular staining in computed tomography before transarterial embolization (A, arrow), but successful necrotization was achieved using transarterial embolization, as shown in this enhanced computed tomographic imaging 1 week after the treatment (B, arrow). However, the treatment failed to increase the patient's blood glucose level.

prevent the hypoglycemia. TAE was performed on the 20th hospital day. We succeeded in necrotizing the metastases, as shown in Fig. 2. However the hypoglycemia persisted, and then the patient required constant glucose infusions and oral feeding to avoid a hypoglycemic attack (Fig. 1). As shown in Fig. 3A and B, bone scintigraphy revealed a worsening of the bone metastases, compared with images obtained 1 year previously.

^{89}Sr is a novel radiopharmaceutical agent used for the palliation of bone pain from multiple osseous metastases (3). The patient suffered from slight lumbago as a result of the bone metastases, so we attempted to use ^{89}Sr to alleviate her pain and to control her hypoglycemia. In the computed tomography (Fig. 4), the bone metastases showed osteoplastic findings that suggested high sensitivity to ^{89}Sr (4). A 110-MBq dose (2 MBq per kg) of ^{89}Sr was administered by intravenous injection on the 37th hospital day (Fig. 1). One week after the injection, the serum level of alkaline phosphatase was normalized. We were able to confirm the accumulation of ^{89}Sr in metastatic foci that corresponded to bone scintigraphy by using gamma camera (Fig. 3C). Three weeks after the ^{89}Sr injection, we were able to reduce the dose of constant glucose infusion while maintaining a euglycemic status. Six weeks after the injection, she stopped constant glucose infusion and the bone pain was relieved (Fig. 1). The patient was discharged on the 83rd hospital day. Two months after the ^{89}Sr injection, she was hospitalized again for 3 weeks because of a transient liver dysfunction due to a hepatitis C virus infection. Liver dysfunction was improved using conservative treatment. In December 2010, no progression of bone metastases was seen on bone scintigraphy, and the hypoglycemic control was consistently good. The patient received a second ^{89}Sr treatment 1 year after the first ^{89}Sr treatment because of the recurrence of bone pain. After the ^{89}Sr treatment, the bone pain has remained improved until the time of writing. Local

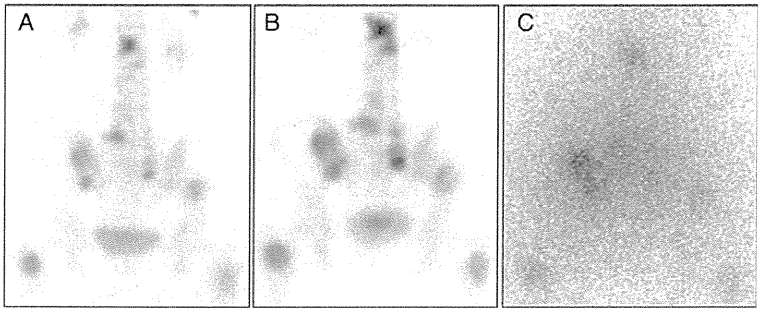

Figure 3. Compared with the results obtained 1 year earlier (A), technetium-99m bone scintigraphy revealed a worsening of the bone metastases (B). The accumulation of strontium-89 in a region corresponding to the observed uptake of sodium pertechnetate was confirmed 1 week after strontium-89 injection (C).

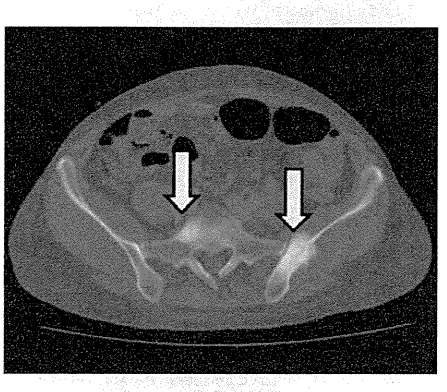

Figure 4. Bone metastases were revealed using computed tomography (arrow).

recurrences of the liver metastases were detected 18 months after TAE (May 2011). Although we proposed additional treatment by TAE or with anticancer agents, the patient refused any additional cancer treatment. At that time, the neuron-specific enolase level was normal (12.1 ng/ml). As of June 2011, the patient continued to be followed up as an outpatient, but she has not received any further treatment for hypoglycemia.

DISCUSSION

Although most patients with malignant insulinoma have lymph node or liver metastasis, there are very few reports in which malignant insulinoma metastasized to a bone (5–7). The prognosis of these patients is relatively poor with a median survival period of ~2 years (8,9).

Glycemic control is a key aspect of managing malignant insulinomas. Mild symptoms can sometimes be controlled by diet (10). Some reports have shown good control of blood glucose levels using a somatostatin analog (11–13). Somatostatin analogs such as octreotide may be helpful for the control of insulin release, but they can also suppress counter-regulatory hormones such as growth hormones, glucagons and catecholamines (10). In this situation, somatostatin analogs can lead to the worsening of hypoglycemia (14). However, octreotide had neither a good nor a bad influence on the hypoglycemia in the patient. Diazoxide, an anti-hypertensive agent known to increase the blood sugar level, inhibits the release of insulin in pancreatic beta cells by opening ATP-sensitive potassium channels (15,16). Its side effects include edema, weight gain, renal impairment and hirsutism (10). Although our patient exhibited edema and weight gain, her hypoglycemia did not improve (Fig. 1). Some authors reported that selective TAE for liver metastases may have the greatest benefit, next to diazoxide (17–22). However, in the present patient, TAE was not effective for glycemic control because unregulated secretion of insulin was mainly caused by the bone metastases.

Concerning other treatment options, De Jong et al. (23) reported that radiolabeled somatostatin analogs, such as [(90)Y-DOTA, Tyr(3)] octreotide and [(177)Lu-DOTA, Tyr(3)] octreotide, are promising treatment modalities for patients with neuroendocrine tumors. However, these radionuclide therapies are not available in Japan. Antiproliferative agents such as streptozotocin, sunitinib and everolimus are also good treatment options (24–26). However, these agents are not covered by the national health insurance in Japan.

^{89}Sr decays by beta emission, with a maximum beta energy of 1.46 MeV, an average soft-tissue penetration of 2.4 mm and a half-life of 50.6 days. After administration, ^{89}Sr is taken up into the mineral matrix of the bone and is selectively concentrated in areas of osteoblastic activity in disease-affected bone, with a biological behavior resembling that of calcium (27). The biodistribution of ^{89}Sr parallels technetium bone-scanning agents (28,29). Pain relief is often obtained 14–21 days after injection (30). Thrombocytopenia and neutropenia are the most common toxic effects, but these effects are generally mild and reversible. Because ^{89}Sr is eliminated mainly via the kidneys, patients are advised to carefully dispose of urine for the first 10 days after administration (27).

The biological mechanism by which ^{89}Sr mediates pain palliation remains unclear. In some basic studies, two possible mechanisms of pain palliation by ^{89}Sr have been proposed (31). One of these mechanisms is a direct radiotoxic effect on the cancer cells caused by the beta-ray emission

from ^{89}Sr. The second mechanism is an indirect action through prostaglandin E2 (PGE2) and interleukin-6 (IL-6) produced by cells in response to ^{89}Sr. PGE2 and IL-6 are known as potent biochemical modifiers of bone turnover. In the patient, the mechanism of improved hypoglycemia was thought to be a direct radiotoxic effect of ^{89}Sr on the cancer cells. The tumoricidal effect of ^{89}Sr on metastatic bone tumors has been reported previously. Dafermou et al. (32) reported that ^{89}Sr therapy resulted in the scintigraphic regression of bone metastases in patients with painful bone metastases from prostate cancer. In addition, Porter et al. (33) reported the reduction of tumor markers, including prostate specific antigen and alkaline phosphatase in the ^{89}Sr therapy of painful bone metastases from prostate cancer. Suzawa et al. (34) reported a case of the complete regression of multiple painful bone metastases from hepatocellular carcinoma after the administration of ^{89}Sr.

In our case, although obvious regression of bone metastases was not detected by the subsequent computed tomography image (Fig. 4), the alkaline phosphatase level decreased (Fig. 1). Because bone scintigraphy was not useful for strict response evaluation, we did not perform it immediately after the strontium-89 injection in this case. Successful pain relief was achieved. Although the intractable hypoglycemia was resistant to all other treatments, it was improved by ^{89}Sr therapy. Though ^{89}Sr therapy is generally indicated for patients with multiple painful bone metastases, in this case, it was also useful as a means of arresting tumor growth and inhibiting tumor activity. To our knowledge, this report is the first to provide evidence that ^{89}Sr can be useful in controlling intractable hypoglycemia in malignant insulinoma with bone metastases.

CONCLUSION

We experienced a case of malignant insulinoma and bone metastases in which intractable hypoglycemia was successfully controlled by using radiopharmaceutical therapy with ^{89}Sr.

Conflict of interest statement

Dr Chigusa Morizane received lecture fee from Novartis Pharma Co., Ltd.

References

1. Vaidakis D, Karoubalis J, Pappa T, Piaditis G, Zografos GN. Pancreatic insulinoma: current issues and trends. *Hepatobiliary Pancreat Dis Int* 2010;9:234–41.
2. Hirshberg B, Cochran C, Skarulis MC, et al. Malignant insulinoma: spectrum of unusual clinical features. *Cancer* 2005;104:264–72.
3. Yamaguchi K. Pain control for bone metastasis using radioactive strontium. *Gan To Kagaku Ryoho* 2010;37:1868–71.
4. Ackery D, Yardley J. Radionuclide-targeted therapy for the management of metastatic bone pain. *Semin Oncol* 1993;20(Suppl. 2):27–31.
5. Sarmiento JM, Que FG, Grant CS, Thompson GB, Farnell MB, Nagorney DM. Concurrent resections of pancreatic islet cell cancers with synchronous hepatic metastases: outcomes of an aggressive approach. *Surgery* 2002;132:976–82.
6. Hesdorffer CS, Stoopler M, Javitch J. Aggressive insulinoma with bone metastases. *Am J Clin Oncol* 1989;12:498–501.
7. Imamura M, Miyashita E, Miyagawa K, Matsuno S, Sato T. Malignant insulinoma with metastasis to gallbladder and bone, accompanied by past history of peptic ulcer and hyperthyroidism. *Dig Dis Sci* 1987;32:1319–24.
8. Danforth DN, Jr, Gorden P, Brennan MF. Metastatic insulin-secreting carcinoma of the pancreas: clinical course and the role of surgery. *Surgery* 1984;96:1027–37.
9. Grama D, Eriksson B, Mårtensson H. Clinical characteristics, treatment and survival in patients with pancreatic tumors causing hormonal syndromes. *World J Surg* 1992;16:632–9.
10. DeVita VT, Jr, Lawrence TS, Rosenberg SA. Chapter 111: Pancreatic neuroendocrine tumors. *Cancer of the Endocrine system/Practice of Oncology DeVita, Hellman, and Rosenberg's Cancer Principles & Practice. 9th edn.* Lippincott: Williams & Wilkins 2011;1489–502.
11. Stefanini P, Carboni M, Patrassi N, Basoli A. Beta-islet cell tumors of the pancreas: results of a study on 1,067 cases. *Surgery* 1974;75:597–609.
12. Baldelli R, Ettorre G, Vennarecci G, et al. Malignant insulinoma presenting as metastatic liver tumor. Case report and review of the literature. *J Exp Clin Cancer Res* 2007;26:603–7.
13. Vezzosi D, Bennet A, Courbon F, Caron P. Short- and long-term somatostatin analogue treatment in patients with hypoglycaemia related to endogenous hyperinsulinism. *Clin Endocrinol (Oxf)* 2008;68:904–11.
14. Stehouwer CD, Lems WF, Fischer HR, Hackeng WH, Naafs MA. Aggravation of hypoglycemia in insulinoma patients by the long-acting somatostatin analogue octreotide (Sandostatin). *Acta Endocrinol (Copenh)* 1989;121:34–40.
15. Fajans SS, Floyd JC, Jr, Knopf RF, Rull J, Guntsche EM, Conn JW. Benzothiadiazine suppression of insulin release from normal and abnormal islet tissue in man. *J Clin Invest* 1966;45:481–92.
16. Fajans SS, Floyd JC, Jr, Thiffault CA, Knopf RF, Harrison TS, Conn JW. Further studies on diazoxide suppression of insulin release from abnormal and normal islet tissue in man. *Ann N Y Acad Sci* 1968;150:261–80.
17. Nesović M, Cirić J, Radojković S, Zarković M, Durović M. Improvement of metastatic endocrine tumors of the pancreas by hepatic artery chemoembolization. *J Endocrinol Invest* 1992;15:543–7.
18. Winkelbauer FW, Nierderle B, Graf O, et al. Malignant insulinoma: permanent hepatic artery embolization of liver metastases—preliminary results. *Cardiovasc Intervent Radiol* 1995;18:353–9.
19. Brown KT, Koh BY, Brody LA, et al. Particle embolization of hepatic neuroendocrine metastases for control of pain and hormonal symptoms. *J Vasc Interv Radiol* 1999;10:397–403.
20. Kim YH, Ajani JA, Carrasco CH, et al. Selective hepatic arterial chemoembolization for liver metastases in patients with carcinoid tumor or islet cell carcinoma. *Cancer Invest* 1999;17:474–8.
21. Moscetti L, Saltarelli R, Giuliani R, Fornarini G, Bezzi M, Cortesi E. Intra-arterial liver chemotherapy and hormone therapy in malignant insulinoma: case report and review of the literature. *Tumori* 2000;86:475–9.
22. Hayashi M, Takaichi K, Kariya T, et al. Malignant insulinoma which expressed a unique creatine kinase isoenzyme: clinical value of arterial embolization as a palliative therapy. *Intern Med* 2000;39:474–7.
23. De Jong M, Valkema R, Jamar F, et al. Somatostatin receptor-targeted radionuclide therapy of tumors: preclinical and clinical findings. *Semin Nucl Med* 2002;32:133–40.
24. Moertel CG, Lefkopoulo M, Lipsitz S, Hahn RG, Klaassen D. Streptozocin-doxorubicin, streptozocin-fluorouracil or chlorozotocin in the treatment of advanced islet-cell carcinoma. *N Engl J Med* 1992;326:519–23.
25. Raymond E, Dahan L, Raoul JL, et al. Sunitinib malate for the treatment of pancreatic neuroendocrine tumors. *N Engl J Med* 2011;364:501–13.
26. Yao JC, Shah MH, Ito T, et al. Everolimus for advanced pancreatic neuroendocrine tumors. *N Engl J Med* 2011;364:514–23.
27. Lin A, Ray ME. Targeted and systemic radiotherapy in the treatment of bone metastasis. *Cancer Metastasis Rev* 2006;25:669–75.

28. Blake GM, Zivanovic MA, McEwan AJ, Ackery DM. Sr-89 therapy: strontium kinetics in disseminated carcinoma of the prostate. *Eur J Nucl Med* 1986;12:447–54.
29. Blake GM, Zivanovic MA, Blaquiere RM, Fine DR, McEwan AJ, Ackery DM. Strontium-89 therapy: measurement of absorbed dose to skeletal metastases. *J Nucl Med* 1988;29:549–57.
30. Lewington VJ, McEwan AJ, Ackery DM, et al. A prospective, randomised double-blind crossover study to examine the efficacy of strontium-89 in pain palliation in patients with advanced prostate cancer metastatic to bone. *Eur J Cancer* 1991;27:954–8.
31. Davis J, Pither RJ. Biochemical responses in cultured cells following exposure to (89)SrCl(2):potential relevance to the mechanism of action in pain palliation. *Eur J Cancer* 2001;37:2464–9.
32. Dafermou A, Colamussi P, Giganti M, Cittanti C, Bestagno M, Piffanelli A. A multicentre observational study of radionuclide therapy in patients with painful bone metastases of prostate cancer. *Eur J Nucl Med* 2001;28:788–98.
33. Porter AT, McEwan AJ, Powe JE, et al. Results of a randomized phase-III trial to evaluate the efficacy of strontium-89 adjuvant to local field external beam irradiation in the management of endocrine resistant metastatic prostate cancer. *Int J Radiat Oncol Biol Phys* 1993;25:805–13.
34. Suzawa N, Yamakado K, Takaki H, Nakatsuka A, Takeda K. Complete regression of multiple painful bone metastases from hepatocellular carcinoma after administration of strontium-89 chloride. *Ann Nucl Med* 2010;24:617–20.

Acta Med. Okayama, 2011
Vol. 65, No. 6, pp. 395-402

Acta Medica Okayama
http://escholarship.lib.okayama-u.ac.jp/amo/

Original Article

The Usefulness of Pre-Radiofrequency Ablation SUV_{max} in ^{18}F-FDG PET/CT to Predict the Risk of a Local Recurrence of Malignant Lung Tumors after Lung Radiofrequency Ablation

Sosuke Harada[a]*, Shuhei Sato[a], Etsuji Suzuki[b], Yoshihiro Okumura[a], Takao Hiraki[a], Hideo Gobara[a], Hidefumi Mimura[a], Susumu Kanazawa[a], Mitsumasa Kaji[c], and Toshiyoshi Fujiwara[d]

Departments of [a]Radiology, [b]Epidemiology, [d]Gastroenterological Surgery, Okayama University Graduate School of Medicine, Dentistry and Pharmaceutical Sciences, Okayama 700-8558, Japan, and [c]Okayama Diagnostic Imaging Center, Okayama 700-0913, Japan

The aim of the present study was to assess the diagnostic usefulness of Fluorine-18 fluorodeoxyglucose (^{18}F-FDG) positron emission tomography/computed tomography (PET/CT) in the prediction of local recurrence of malignant lung tumors by analyzing the pre-radiofrequency ablation (RFA) maximal standardized uptake value (SUV_{max}). We performed a historical cohort study of consecutive malignant lung tumors treated by RFA from January 2007 to May 2008 at Okayama University Hospital. We selected only lung tumors examined by PET/CT within 90 days before RFA and divided them (10 primary and 29 metastatic) into 3 groups according to their tertiles of SUV_{max}. We calculated recurrence odds ratios in the medium group and the high group compared to the low group using multivariate logistic analysis. After we examined the relationship between SUV_{max} and recurrence in a crude model, we adjusted for some factors. Tumors with higher SUV_{max} showed higher recurrence odds ratios (medium group; 1.84, high group; 4.14, respectively). The tumor size also increased the recurrence odds ratio (2.67); we thought this was mainly due to selection bias because we excluded tumors less than 10 mm in diameter. This study demonstrated the pre-RFA SUV_{max} in PET/CT may be a prognostic factor for local recurrence of malignant lung tumors.

Key words: fluorodeoxyglucose (FDG), positron emission tomography (PET), standardized uptake value (SUV), radiofrequency ablation (RFA), lung

Radiofrequency ablation (RFA) is a thermal therapy that results in coagulation tumor necrosis and can be used to treat malignant lung tumors. Preliminary studies of the use of RFA to treat lung tumors have shown promising results for initial local control in carefully selected patient populations [1-6].

Received March 30, 2011; accepted September 7, 2011.
*Corresponding author. Phone:+81-86-235-7313; Fax:+81-86-235-7316
E-mail:radiol@cc.okayama-u.ac.jp (S. Harada)

Fluorine-18 fluorodeoxyglucose (^{18}F-FDG) positron emission tomography/computed tomography (PET/CT) is a noninvasive, convenient, and feasible tool that is now integral to the management of various cancers. PET/CT is also a valuable technique for evaluating local control after radiotherapy or prognostic long-term outcome after surgery, chemotherapy or radiotherapy for several cancers [7-13]. This use is sometimes even more important than its ability to be used as an anatomic imaging modality to detect distant metastases and identify remote recurrent disease

[14].

The standardized uptake value (SUV) of FDG is the ratio of activity in tissue per unit volume to the activity in the injected dose per patient body weight, and it is widely used because of its simplicity. The SUV_{max} is the maximal value of the SUV in a tumor section.

It has been reported that the increased expression of glucose transporters in malignant cells may be associated with a higher metabolism and increased rates of glucose utilization in non-small cell lung cancer [15]; therefore, tumor proliferation, progression and metastasis are associated with the SUV [16, 17]. This indicates that the SUV_{max} might reflect the malignant potential in lung tumors.

The aim of this study was to assess the diagnostic utility of PET/CT for the prediction of local tumor recurrence by analyzing the pre-RFA SUV_{max} in primary lung cancers or metastatic malignant lung tumors.

Materials and Methods

The institutional review board of Okayama University Hospital approved the study and informed consent was obtained from all patients before they underwent lung RFA.

The method used for patient selection is shown in Fig. 1. This study included 251 consecutive lung tumors that were treated by lung RFA with multi-

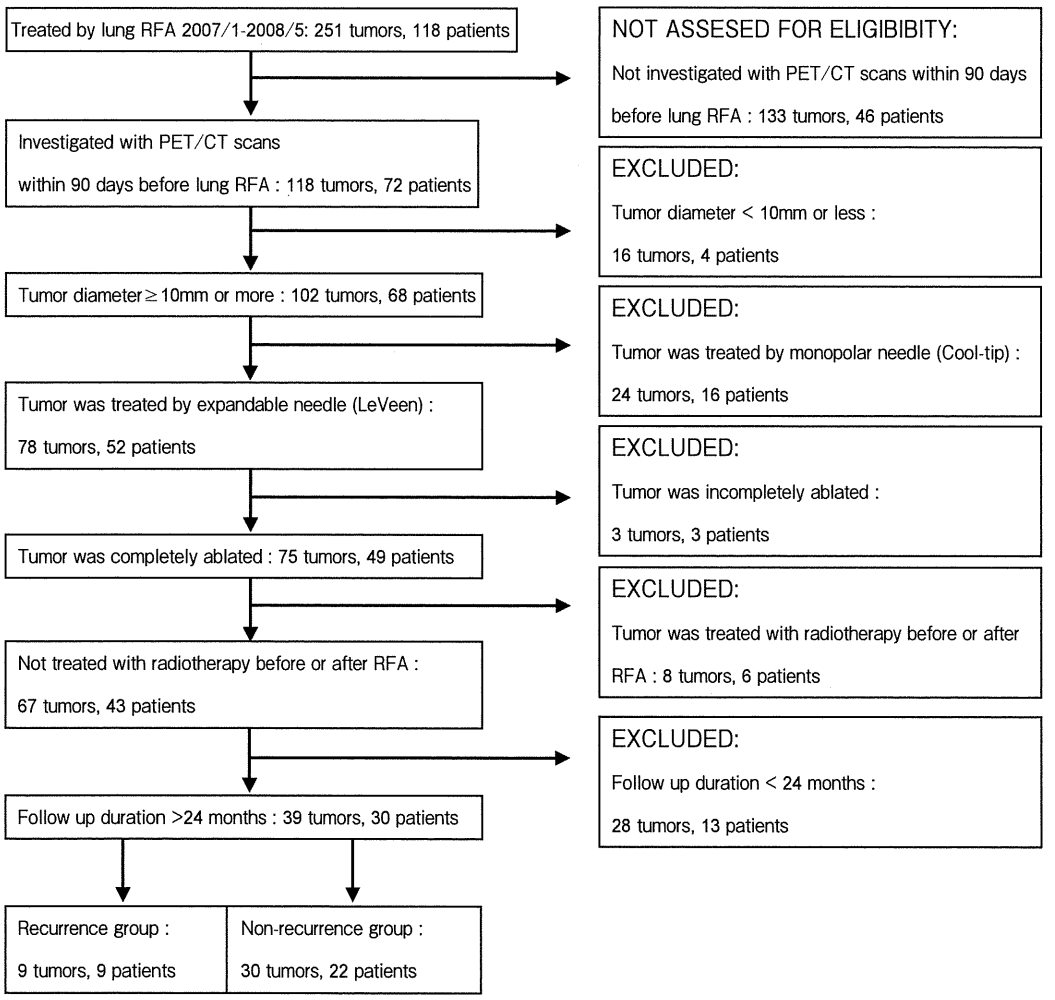

Fig. 1 A flowchart depicting the patient selection. ※Sometimes there were multiple nodules in the same patient.

tined expandable electrodes from January 2007 to May 2008 at Okayama University Hospital. We then selected only tumors that were investigated using PET/CT scans within 90 days before lung RFA. Whole-body pre-RFA PET/CT was performed as a routine examination for most of these patients. We excluded tumors less than 10 mm in diameter (their maximum diameters were measured on pulmonary window setting CT images). We also excluded tumors ablated with a single internally cooled electrode (Cool-tip; Covidien, Mansfield, MA, USA), ablated incompletely, or treated with radiotherapy before or after RFA. Some patients underwent systemic chemotherapy before lung RFA (14 patients, 20/39 tumors) or after lung RFA (11 patients, 15/39 tumors). We did not exclude these tumors treated by chemotherapy before and after RFA. No concurrent chemotherapy was administered within the treatment period of the lung RFA. For the recurrent group, we stopped following up patients when tumor recurrence was found. For the non-recurrent group, we excluded tumors for which the follow-up duration was less than 24 months; in order to distinguish non-recurrent tumors from recurrent tumors. The mean follow-up duration was 29.5 ± 4.1 mo (range, 24.1–36.7 mo) in the nonrecurrence group. Finally, the selected tumors consisted of 10 primary lung cancers and 29 metastatic malignant lung tumors (mean size, 16.4 mm). The patients consisted of 17 males and 12 females (mean age, 68.0 years).

Those tumors comprised 5 tumor types: primary lung cancer (n = 10), pulmonary metastases from lung cancer (n = 3), colorectal cancer (n = 19), hepatocellular carcinoma (n = 5), and leiomyosarcoma (n = 2). The characteristics of the patients are summarized in Table 1.

PET/CT was performed a mean of 19.3 ± 21.7 d (range 1–83 d) before lung RFA, using a PET/CT scanner (Biograph LSO/Sensation 16, Siemens, Munich, Germany). After fasting for at least 5 h, patients were injected with 3.7 MBq (megabecquerel) of ^{18}F-FDG *per kg* (kilogram) of body weight, and images were acquired 1.5 h later. On arrival at our hospital, their serum glucose was checked before ^{18}F-FDG injection, and was less than 200 mg/dl in all patients. Emission scanning was performed from the skull base to the proximal thigh, and afterward, the CT scanned voxel value was used for attenuation correction. Images were reconstructed using an iterative reconstruction algorithm (ordered-subset expectation maximization: OSEM). The technical parameters for the 16-detector row helical CT included a section thickness of 3 mm in the soft tissue window and 5 mm in the lung window, a pitch factor of 0.8 (1.5 mm × 16 collimation, mm/rotation = 19.2) and a gantry rotation speed of 0.5 s (Care dose 4D, 50 mAs).

Table 1 Characteristics of the patients

Gender (the number of patients)	
Male : Female	17 : 12
Age	
Mean:	68.0
Median:	69.0
Range:	51–87
Histology (the number of tumors)	
Primary Lung Neoplasm (10)	
Squamous	1
Adenocarcinoma	5
NSCLC[1], not specified	4
Recurrent Lung Neoplasm (3)	
Squamous	1
Adenocarcinoma	2
Metastatic (26)	
Colorectal cancer	19
Hepatocellular carcinoma	5
Leiomyosarcoma	2
Chemotherapy	
Yes	15
No	14

[1]NSCLC, Non-small cell lung cancer.

For the regions of interest (ROI), the images were transferred to the workstation (Fujin-Raijin, AZE Inc., Tokyo, Japan), and FDG-PET scans were analyzed by 2 experienced nuclear physicians who were blinded to the histopathological findings and clinical follow-up data. To evaluate the ^{18}F-FDG uptake, they drew ROI for tumors and measured the SUV_{max} in each ROI using the Fujin-Raijin software program.

During the follow-up, CT or PET/CT was performed approximately 1, 3, 6, 9, 12 and then every 6 months after lung RFA. Local control was evaluated with CT. We compared the tumor size and the geometry of the ablation zone with the previous CT images. Local tumor progression was considered to have occurred when the ablation zone was circumferentially enlarged compared to the previous CT images. The appearance of an irregular, scattered, nodular, or eccentric focus in the ablation zone on contrast-

enhanced CT was also considered to indicate local progression [4, 18].

We calculated the SUV_{max} and tumor size for each tumor. To assess to what extent the other most often-quoted prognostic factors have an effect on tumor recurrence, we added 6 other major tumor characteristics which might have affected the tumor recurrence, including: age, sex (male or female), chemotherapy (yes or no), primary or metastatic disease, the interval between PET/CT and RFA execution, and proximity (yes or no; whether or not a tumor was in contact with a large blood vessel or bronchus; if those tumors were contiguous with a vessel of diameter ≥ 3mm or a bronchus with an inner diameter ≥2mm, we considered the tumor to have proximity) to the statistical analyses.

Statistical analysis. We divided the tumors into 3 groups according to the tertile of the SUV_{max} value, a low group ($SUV_{max} \leq 2.54$), medium group ($2.54 < SUV_{max} \leq 4.61$) and a high group ($SUV_{max} \geq 4.61$) and performed a descriptive statistical analysis of the tumor characteristics. We calculated the odds ratios and their 95% confidence intervals for recurrence in the tumor group with high SUV_{max} values compared to the tumor group with low SUV_{max} values using multivariate logistic regression analysis. After we examined the relationship between SUV_{max} and recurrence in a crude model, we adjusted for sex and age (model 1), proximity (model 2), and, finally, tumor size (model 3). We also calculated the Spearman's correlation coefficient between the tumor size and SUV_{max}.

We considered a p-value < 0.05 (two-sided test) to be a statistically significant difference. All statistical analyses were performed by using the SPSS 17.0 for Windows software package (SPSS, Inc., Chicago, IL, USA).

Results

During the follow-up period, tumor recurrences were observed in 9 of 39 tumors (23.1%). Three recurrences occurred within the first 6 months, another 5 within the next 6 months, and 1 at 31 months after lung RFA.

Among the 3 tumor groups established according to the SUV_{max} values, only the tumor size was significantly different (Table 2).

Table 2 Comparison of descriptive statistics

Tumor characteristics		Low	Medium	High	*P*-value
		$SUV_{max} \leqq 2.54$ (n = 13)	$2.54 < SUV_{max} \leqq 4.61$ (n = 13)	$SUV_{max} > 4.61$ (n = 13)	
Chemotherapy	Yes	9	9	10	0.88
	No	4	4	3	
Tumor size (mm)	Mean ± SD	13.9 ± 6.1	16.9 ± 5.5	18.5 ± 7.7	0.049*
Primary or metastatic	Primary	4	3	3	0.88
	Metastatic	9	10	10	
PET/CT-RFA interval (days)	Mean ± SD	29.8 ± 29.4	16.8 ± 15.7	11.3 ± 13.5	0.41
Proximity	Yes	1	2	3	0.56
	No	12	11	10	
Recurrence	Yes	1	3	5	0.18
	No	12	10	8	

PET/CT, positron emission tomography/computed tomography; RFA, radiofrequency ablation; SD, standard deviation; SUV_{max}, maximal standardized uptake value.

P-values were calculated using the upper-sided Kruskal-Wallis test and $p < .05$ was considered to represent statistical significance, as indicated by*.

Adjusting for sex, age, proximity, and tumor size, we found that higher SUV_{max} was associated with higher odds ratios for recurrence (medium group: 1.84; high group: 4.14) compared with the low group (Table 3, model 3). Other factors that increased the odds ratios for recurrence were gender (being male; odds ratios=4.38) and tumor size (odds ratio = 2.67), although their 95% confidence intervals were quite wide. Regarding age and proximity, however, we found no clear association with the odds ratios for recurrence (odds ratios = 1.06, 0.84, respectively).

The Spearman's correlation coefficient between the tumor size and SUV_{max} was 0.456 ($p = 0.004$), indicating that the tumor size and SUV_{max} were in moderate correlation. Fig. 2A and 2B show a recurrence case, whereas Fig. 3A and 3B show a non-recurrence case.

Discussion

In many institutes, ^{18}F-FDG PET/CT has been used to assess the presence of whole body metastases before and after lung RFA. Although the SUV_{max} has been suggested to be helpful in predicting the risk of local recurrence after radiotherapy in lung cancer and other several cancers [7, 8], it has not been fully verified whether the pre-RFA SUV_{max} is capable of predicting the risk of local recurrence after lung RFA. This historical cohort study examined whether the pre-RFA SUV_{max} can be useful to predict the risk of local recurrence after lung RFA. We demonstrated that, in addition to its original diagnostic purpose, ^{18}F-FDG PET/CT could also provide a prognostic factor for local tumor recurrence after lung RFA.

Table 3 Odds ratios and 95% confidence intervals for recurrence

		Crude model		Model 1		Model 2		Model 3	
		OR	(95% CI)	OR	(95% CI)	OR	(95% CI)	OR	(95% CI)
SUV_{max}	Low	1.00		1.00		1.00		1.00	
	Medium	3.60	(0.32-40.23)	2.22	(0.18-28.18)	2.25	(0.17-29.41)	1.84	(0.13-25.41)
	High	7.50	(0.73-76.77)	5.26	(0.45-62.12)	5.33	(0.43-65.62)	4.14	(0.31-54.44)
Sex	Male			4.35	(0.36-52.69)	4.33	(0.36-52.69)	4.38	(0.38-50.58)
Age	(1 year)			1.06	(0.94-1.21)	1.07	(0.94-1.21)	1.06	(0.94-1.20)
Proximity						0.94	(0.11-8.17)	0.84	(0.09-7.77)
Tumor size ≥15mm								2.67	(0.39-18.54)

CI, confidence interval; OR, odds ratio; SUV_{max}, maximal standardized uptake value.

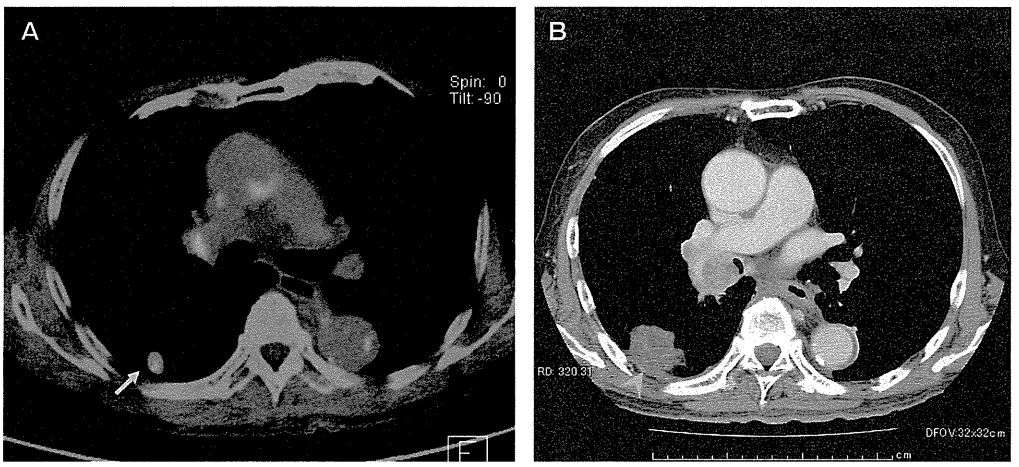

Fig. 2 **A**, Pre-RFA PET/CT of a 77-year-old male with local recurrence. The PET/CT showed primary lung cancer (adenocarcinoma) in the right lower lobe (oblique arrow). This tumor was treated by RFA. The SUV_{max} of the tumor was 3.89; **B**, The follow-up CT examination was performed 9 months after RFA. The contrast-enhanced CT showed local tumor progression. The ablation zone was circumferentially enlarged. Also, an irregular focus appeared in the ablation zone on contrast-enhanced CT (arrow head).

This result was in agreement with a similar study by Singnurkar *et al.* [20]. Our study was performed strictly using only subjects whose tumors were treated with a LeVeen Needle Electrode (Boston Scientific Japan Corp., Tokyo, Japan). We also reviewed the most effective prognostic factors of those currently reported and investigated their prognostic value in predicting local tumor recurrence.

Hiraki T. *et al.* previously reported that the overall local control rates of malignant primary lung cancer and pulmonary metastasis after lung RFA were 97%, 86%, 81%, and 76% at 6, 12, 18, and 24 months, respectively [19]. In other words 24% of malignant lung tumors recur within 2 years after RFA.

Although pre-RFA ^{18}F-FDG uptake in lung tumors might not be a direct indicator of residual micrometastases after RFA, we expected that ^{18}F-FDG uptake might be correlated with the malignant potential of tumor cells. The pre-RFA SUV_{max} in tumors reflects their glucose metabolism, which is facilitated in the most malignant tumors. This parameter may lead to a better understanding of the malignant potential of the tumor, and therefore, can be used to predict the risk of local tumor recurrence after lung RFA. Our results indicate that when the pre-RFA SUV_{max} is high, the risk of recurrence is high.

The other factors associated with higher odds ratios for recurrence were gender (being male; odds ratio = 4.38) and tumor size (odds ratio = 2.67). With regard to the tumor size, we calculated the odds ratio for the recurrence of tumors with a diameter ≥ 15 mm compared to tumors with a diameter < 15 mm. Note that, however, there were many tumors from male patients in the recurrence group (8/9) and that there were only 2 tumors of < 15 mm in the recurrence group (2/9) because tumors < 10 mm in diameter were excluded from this study. Thus, the present findings should be carefully interpreted in light of a possible selection bias.

Various studies have shown that tumor size is a very important factor in predicting the local control of lung tumors after RFA [20-23]. Many studies have also reported that the SUV_{max} values of tumors are associated with their pathological diameter [24-26]. This may indicate that the SUV_{max} and the tumor size measured on CT will be correlated. A Spearman's test of our present data supported this hypothesis, and showed that the tumor size and SUV_{max} had a moderate correlation (correlation coefficient = 0.456, $p = 0.004$).

There were several limitations to this study. First, all of the cases of primary lung cancer were diagnosed on the basis of histological evidence. However, most of the cases of pulmonary metastases were diagnosed only by CT without histological evidence; they had surgically or biopsy-proven primary cancers, and the diagnoses of lung metastasis and local progressions after RFA were only based on radiological images. The second limitation is that the number of cases was

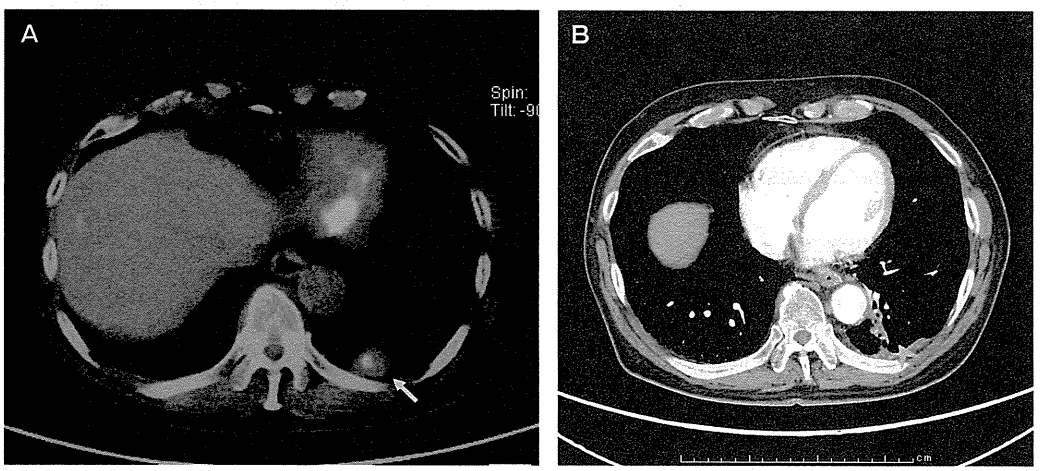

Fig. 3 **A**, Pre-RFA PET/CT of a 67-year-old male without local recurrence. The PET/CT showed a metastatic lesion in the left lung from primary rectal cancer (oblique arrow). The metastatic tumor was treated by RFA. The SUV_{max} in the tumor was 2.36; **B**, The follow-up CT examination was performed 25 months after RFA. The contrast-enhanced CT shows no irregular enhancement (arrow head).